

NUMERICAL STUDY OF A MATHEMATICAL MODEL OF A FREE-SURFACE POTENTIAL FLOW

SERGUINE HOURIA, GUECHI FAIROUZ, AND GASMI ABDELKADER

Received 16 November, 2022; accepted 28 March, 2023; published 28 April, 2023.

DEPARTMENT OF MATHEMATICS, FACULTY OF SCIENCE, FERHAT ABBAS UNIVERSITY,
19000, SETIF, ALGERIA.

houria.serguine@univ-msila.dz

DEPARTMENT OF MATHEMATICS, FACULTY OF SCIENCE, FERHAT ABBAS UNIVERSITY,
19000, SETIF, ALGERIA.

fairouz.chegaar@univ-setif.dz

LABORATORY OF PURE AND APPLIED MATHEMATICS, FACULTY OF MATHEMATICS AND
COMPUTER SCIENCE, MOHAMED BOUDIAF UNIVERSITY, 28000, M'SILA, ALGERIA.

abdelkader.gasmi@univ-msila.dz

ABSTRACT. In this work, the problem of a potential and two-dimensional flow with a free surface of an incompressible, irrotational and inviscid fluid of a jet in front an inclined wall is considered, where γ is the inclination angle with the horizontal. The shape of the free surface is presented by curves which are found numerically by the series truncation method. This technique is based on the conformal transformations, resulting with the surface tension effect T with the boundary conditions on the free surfaces given by Bernoulli's equation. The found results are dependant on parameters which are: the Weber's number α and the angle γ . For each Weber's number value, only one solution is specified and some shapes of free surfaces of the jet are illustrated.

Key words and phrases: Free surface; Potential flow; Surface tension; Weber number; Series truncation method.

2010 Mathematics Subject Classification. Primary 76A02, 76B07, 76B10. Secondary 30C30, 30C35, 65D25.

1. INTRODUCTION

One considers the study of a two-dimensional and potential flow of a jet in front of an inclined wall by γ , where γ is the inclination angle with the horizontal. The fluid is assumed to be as incompressible, irrotational and inviscid. The application of the hodograph transformation method to the jet theory can be found by Birkoff and Zarantonello [4], some generalizations of the Schwartz Christoffel formula are given by this method [6] and [8] which transforms a half of a field occupied by a flow into a field with a border which combines a polygon and smooth curve. A various flow studies were presented by many authors [10], [5], [7] and [9]. Jets impinging on the walls were studied by many authors [13]. Weidong Peng and David F.Parker assumed a jet of fluid jet hitting an irregular wall [13]. The authors assumed different smooth wall geometries in their paper, neglecting the effects of the surface tension and the gravity, the problem can be transformed to an integral equation on the free boundary that they solved numerically. In this paper, we consider the same problem as it is proposed, but we take into account the tension surface effect with neglecting the effect of gravity and the shape of the free surface constituted by the flow is studied. Far upstream the flow velocity is a constant \tilde{U} and the fluid depth is $2\tilde{H}$. This problem is characterized by the nonlinear boundary condition given by Bernoulli's equation on free surfaces which are not of known shape. In this case, a series truncation procedure is used to calculate the numerical solutions of the flow in front of a wall. This method has been used with success by Birkoff, Zarantonello [4] and many authors like [1, 2, 3] and [11, 12] to obtain the calculation of the nonlinear free surface flow and bow flow. we take note that the flow is characterized by two parameters; the first is the angle γ between the horizontal bottom and the inclined wall and the second is the Weber number α ; This number is defined by

$$(1.1) \quad \alpha = \frac{\tilde{\rho} \tilde{U}^2 \tilde{H}}{\tilde{T}}.$$

Here, \tilde{T} is the surface tension, and $\tilde{\rho}$ is the density of the fluid. The problem is given and formulated in section 2, the numerical procedure is presented in section 3 and the results that are obtained, are discussed in section 4.

2. MATHEMATICAL FORMULATION

One proposes a potential and two-dimensional flow of a jet of an incompressible and inviscid fluid. On the free surface in front of a wall inclined by an angle γ made up with the horizontal one, the gravity's effect is neglected and only the surface tension effect can be taken into consideration. And like locates coordinates, one takes wall EO on the axis $\tilde{x}o\tilde{x}'$ and wall COC' on the line of the equation $\tilde{y} = -\tan(\gamma)$. It is supposed that when $\tilde{x} \rightarrow -\infty$, the flow is uniform with the velocity \tilde{U} and the depth $2\tilde{H}$. The flow is limited in an upper by the streamline AB and in a lower position by the streamline $A'B'$, and the speed has a proportional relationship with \tilde{x} , because when $\tilde{x} \rightarrow 0$, the speed tends towards zero, (see Figure 1).

We define the complex variable $\tilde{z} = \tilde{x} + i\tilde{y}$. The complex conjugate velocity is given by $\tilde{\xi} = \tilde{u} - i\tilde{v}$, where \tilde{u} and \tilde{v} are respectively the components of the fluid velocity and by $\tilde{f} = \tilde{\phi} + i\tilde{\psi}$ the potential function complexes, where $\tilde{\phi}$ and $\tilde{\psi}$ respectively indicate the potential function and the function of current. One chooses $\tilde{\phi} = 0$ at the point $(\tilde{x}, \tilde{y}) = (0, 0)$ and $\tilde{\psi} = 0$ on the streamline EOC (EOC'), it follows that $\tilde{\psi} = \tilde{U}\tilde{H}$, $\tilde{\psi} = -\tilde{U}\tilde{H}$ on the streamline ADB and

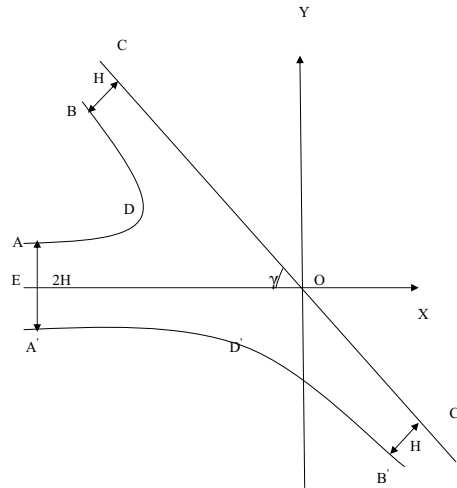


Figure 1: Flow in the z-plane

$A'D'B'$. Under these conditions the equation of Bernoulli on the free surfaces is given by

$$(2.1) \quad \frac{1}{2} \tilde{q}^2 + \frac{\tilde{P}}{\tilde{\rho}} = C, \text{ on } ADB \text{ and } A'D'B'$$

Where \tilde{P} is the pressure of the fluid, $\tilde{\rho}$ is the density of the fluid and $\tilde{q} = \sqrt{\tilde{u}^2 + \tilde{v}^2}$ indicates the module speed. Just above the free surface, we consider

$$\tilde{P}_0$$

is considered to be constant. Since far upstream the free surface is horizontal, we have $\tilde{P} = \tilde{P}_0$. Thus, the constant C in the equation is evaluated far upstream and is given by

$$(2.2) \quad \frac{1}{2} \tilde{U}^2 + \frac{\tilde{P}_0}{\tilde{\rho}} = C.$$

Laplace's formula gives the relation between \tilde{P} and \tilde{P}_0 as

$$(2.3) \quad \tilde{P} - \tilde{P}_0 = -\tilde{T}\tilde{K}.$$

Where \tilde{K} is the curvature of the free surface and \tilde{T} is the surface tension. And by substitution (2.3) into (2.2) we obtain

$$(2.4) \quad \frac{1}{2} \tilde{q}^2 - \frac{\tilde{T}}{\tilde{\rho}} \tilde{K} = \frac{1}{2} \tilde{U}^2.$$

We introduce the dimensionless variables by taking \tilde{H} as the unit length and \tilde{U} as the unit velocity. The dimensionless variables are given by

$$(2.5) \quad x = \frac{\tilde{x}}{\tilde{H}}, y = \frac{\tilde{y}}{\tilde{H}}, q = \frac{\tilde{q}}{\tilde{U}}, K = \tilde{H} \tilde{R}, C = \frac{\tilde{y}_c}{\tilde{H}}.$$

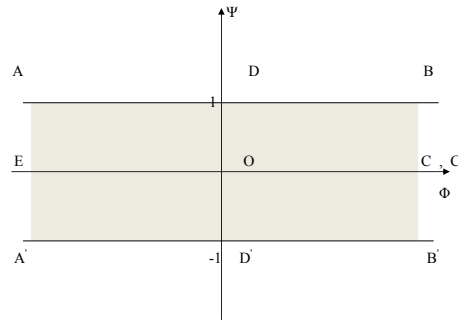


Figure 2: Potential flow in the potential f -plane

The dimensionless parameter C has a particular property; it gives the value of the ratio of the depth of the nearest point on the free surface at the stagnation point O to the depth of the fluid at infinity, this ratio defines the coefficient of contraction. The dimensionless complex potential function and the dimensionless complex velocity are given by

$$f = \phi + i\psi \quad \text{and} \quad \xi = \frac{df}{dz} = u - iv.$$

Hence

$$u = \frac{\partial \phi}{\partial x} = \frac{\partial \psi}{\partial y} \quad \text{and} \quad v = \frac{\partial \phi}{\partial y} = -\frac{\partial \psi}{\partial x}.$$

ϕ is the dimensionless potential function, ψ is the dimensionless stream (see Figure 2).

In the dimensionless form, the Bernoulli equation (2.4) becomes

$$(2.6) \quad q^2 - \frac{2}{\alpha}K = 1.$$

Here α is the Weber number defined in (1.1).

The physical flow problem as described above can be formulated as a boundary value problem in the potential function $\phi(x, y)$

$$(2.7) \quad \begin{cases} \Delta \phi = 0, & \text{in the flow domain.} \\ \frac{\partial \phi}{\partial \theta} = 0, & \text{on the rigid boundary.} \\ |\Delta \phi|^2 - \frac{2}{\alpha}K = 1, & \text{on the free surface.} \\ \phi(0, 0) = 0. \end{cases}$$

Solving the problem in this form is very difficult specially that the nonlinear boundary condition is specified on an unknown boundary (the free surface). Instead of solving the problem in its partial differential equation form in ϕ , we take advantage of the property that for the bidimensional potential flow (as is in our problem) and if the plane in which the flow is embedded is identified to the complex plane, the complex velocity $\xi = u - iv$ and the complex potential function $f = \phi + i\psi$ are analytic functions of the complex variable $z = x + iy$. Hence, we use all the necessary properties of analytic functions of a complex variable: integral formulation, conform transformation. Because $(u - iv)$ is analytical, one defines the function $(\tau - i\theta)$ by the relation

$$(2.8) \quad \xi = u - iv = \tau - i\theta.$$

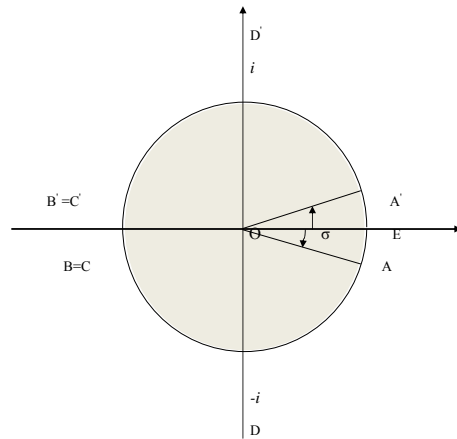


Figure 3: Flow in the t -plane

θ is the angle between the flight path vector and the horizontal one. Hence, equation (2.5) becomes

$$(2.9) \quad \frac{1}{2}q^2 - \frac{1}{\alpha}q \left| \frac{\partial\theta}{\partial\phi} \right| = \frac{1}{2}, \quad \text{on } ADB \text{ and } A'D'B'$$

It is known that $\theta(\phi)$ is an increasing function when $-\infty < \phi < +\infty$ on the free surfaces. The equation of Bernoulli in the f -plane is written

$$(2.10) \quad \frac{1}{2} \exp(2\tau) - \frac{1}{\alpha} \exp(\tau) \left| \frac{\partial\theta}{\partial\phi} \right| = \frac{1}{2}, \quad \text{on } ADB \text{ and } A'D'B'$$

With the conditions

$$(2.11) \quad \begin{cases} \theta = 0, \psi = 0, \phi < 0, & \text{on } EO \\ \theta = \gamma, \psi = 0, \phi > 0, & \text{on } OC \\ \theta = \pi - \gamma, \psi = 0, \phi > 0, & \text{on } OC' \end{cases}$$

This mathematical problem is to determine the function $\tau - i\theta$ which is analytical in the band $-1 < \psi < 1$ and which checks the conditions (2.10) and (2.11).

3. NUMERICAL PROCEDURE

We go to the step which we use the technique of truncation of the series. Using the Schwartz-Christoffel transformation, we map the strip $-1 < \psi < 1$ in the f -plane into a disc unit in the t -plane by the transformation

$$(3.1) \quad f = \frac{2}{\pi} \ln \left(\frac{1-t}{1+t} \right).$$

The points (A, E, A') ; (B, C, B', C') ; $D; D'$ and O in the f -plane are respectively transformed at $t = 1, t = -1, t = -i, t = i$ and $t = 0$.

The free surface's points in the t plane are given by

$$(3.2) \quad t = |t| \exp(i\sigma) = \begin{cases} \exp(i\sigma), & -\pi < \sigma < 0 \text{ on } ADB \\ \exp(i\sigma), & 0 < \sigma < \pi \text{ on } A'D'B' \end{cases}$$

One as follows, writes the Bernoulli equation in the t plane

$$(3.3) \quad \begin{cases} \exp(2\tau) + \frac{\pi}{\alpha} \sin(\sigma) \exp(\tau) \frac{\partial \theta}{\partial \sigma} = 1, & \text{on } AB \\ \exp(2\tau) - \frac{\pi}{\alpha} \sin(\sigma) \exp(\tau) \frac{\partial \theta}{\partial \sigma} = 1, & \text{on } A'B' \end{cases}$$

3.1. Local behavior of ξ at $t = 0$. At the point of stagnation O , when $t = 0$, we have a flow characterized by the following potential functions

$$(3.4) \quad f \sim \begin{cases} a(z)^{\frac{\pi}{\gamma}}, & \text{on } AB \\ a(z)^{\pi - \gamma}, & \text{on } A'B' \end{cases}$$

The development limited of f in the vicinity of the point $t = 0$ is given by

$$(3.5) \quad f \sim t + O(t^2).$$

3.2. Formulation of the series. Lets us define the function $\Omega(t)$ as follows $\xi(t) = g(t) \Omega(t)$, where $g(t)$ contains the singularities and the zeros. The function $\Omega(t)$ is bounded and continuous on the unit circle and analytic in the interior of the unit disc, hence $\Omega(t)$ can be expressed as an exponential of the analytical function inside the disc unit $|t| < 1$. Therefore, we can write $\xi(t)$ as

$$(3.6) \quad \xi(t) = g(t) \exp\left(\sum_{n=0}^{+\infty} a_n t^n\right).$$

By using the conditions and the relations (3.3) and (3.4), the equation (3.5) becomes

$$(3.7) \quad \xi(t) = u - iv = \begin{cases} (t)^{\frac{\pi - \gamma}{\pi}} \exp\left(\sum_{k=0}^{+\infty} a_k t^{2k}\right), & \text{on } AB \\ (t)^{\frac{\gamma}{\pi}} \exp\left(\sum_{k=0}^{+\infty} a_k t^{2k}\right), & \text{on } A'B' \end{cases}$$

By choosing all the coefficients a_k to be real.

The function (3.5) satisfies (2.10) and the coefficients a_k have to be determined to satisfy (2.10).

While using (3.2), (3.7) becomes

$$(3.8) \quad \begin{cases} \exp\left[\sum_{k=0}^{+\infty} a_k \cos(2k\sigma) + i\left(\left(\frac{\pi - \gamma}{\pi}\right)\sigma + \sum_{k=0}^{+\infty} a_k \sin(2k\sigma)\right)\right], & \text{on } AB \\ \exp\left[\sum_{k=0}^{+\infty} a_k \cos(2k\sigma) + i\left(\left(\frac{\gamma}{\pi}\right)\sigma + \sum_{k=0}^{+\infty} a_k \sin(2k\sigma)\right)\right], & \text{on } A'B' \end{cases}$$

From where

$$(3.9) \quad \tau(\sigma) = \sum_{k=0}^{+\infty} a_k \cos(2k\sigma), \text{ on } AB \text{ and } A'B'$$

and

$$(3.10) \quad \theta(\sigma) = \begin{cases} -\left(\left(\frac{\pi - \gamma}{\pi}\right)\sigma + \sum_{k=0}^{+\infty} a_k \sin(2k\sigma)\right), & \text{on } AB \\ -\left(\left(\frac{\gamma}{\pi}\right)\sigma + \sum_{k=0}^{+\infty} a_k \sin(2k\sigma)\right), & \text{on } A'B' \end{cases}$$

The problem can be solved numerically by the truncation of the infinite series after N terms. Introducing the $N + 1$ such points

$$(3.11) \quad \sigma(I) = \begin{cases} -\frac{\pi}{2(N+1)}\left(I - \frac{1}{2}\right), & \text{on } AB \\ \frac{\pi}{2(N+1)}\left(I - \frac{1}{2}\right), & \text{on } A'B' \end{cases} \quad I = 1, 2, \dots, N + 1$$

We find the N coefficients and by collocation using (3.11), we obtain $[\tau(\sigma)]_{\sigma=\sigma(I)}$ and $[\theta(\sigma)]_{\sigma=\sigma(I)}$ in terms of coefficients a_k .

Thus, we obtain N nonlinear algebraic equations of N unknowns ($a_k, k = 0, \dots, N$). Using Newton's method to solve the obtained system.

$$(3.12) \quad \begin{cases} \exp\left(2\sum_{k=0}^N a_k \cos(2k\sigma(I))\right) - \frac{\pi}{\alpha} \exp\left(\sum_{k=0}^N a_k \cos(2k\sigma(I))\right) \\ \times (\sin \sigma(I)) \left(\left(\frac{\pi - \gamma}{\pi}\right)\sigma(I) + \sum_{k=0}^N a_k \sin(2k\sigma(I))\right) = 1, & \text{on } AB \\ \exp\left(2\sum_{k=0}^N a_k \cos(2k\sigma(I))\right) + \frac{\pi}{\alpha} \exp\left(\sum_{k=0}^N a_k \cos(2k\sigma(I))\right) \\ \times (\sin \sigma(I)) \left(\left(\frac{\gamma}{\pi}\right)\sigma(I) + \sum_{k=0}^N a_k \sin(2k\sigma(I))\right) = 1, & \text{on } A'B' \end{cases}$$

To plot the curve of the free surface, we use the following formula

$$(3.13) \quad \frac{\partial x}{\partial \phi} + i \frac{\partial y}{\partial \psi} = \frac{1}{\xi} = \frac{1}{u - iv} = e^{-\tau + i\theta}.$$

After simple calculations, we obtain the following systems of equations

$$(3.14) \quad \begin{cases} \frac{\partial x}{\partial \sigma}(\sigma(I)) = \frac{2C}{\pi \sin \sigma(I)} \exp\left(-\sum_{k=0}^N a_k \cos(2k\sigma(I))\right) \times \\ \cos\left(-\left(\frac{\pi - \gamma}{\pi}\right)\sigma - \sum_{k=0}^N a_k \sin(2k\sigma(I))\right). \\ \frac{\partial y}{\partial \sigma}(\sigma(I)) = \frac{2C}{\pi \sin \sigma(I)} \exp\left(-\sum_{k=0}^N a_k \cos(2k\sigma(I))\right) \times \\ \sin\left(-\left(\frac{\pi - \gamma}{\pi}\right)\sigma - \sum_{k=0}^N a_k \sin(2k\sigma(I))\right). \end{cases} \quad \text{on } AB$$

and

$$(3.15) \quad \left\{ \begin{array}{l} \frac{\partial x}{\partial \sigma}(\sigma(I)) = \frac{2C}{\pi \sin \sigma(I)} \exp\left(-\sum_{k=0}^N a_k \cos(2k\sigma(I))\right) \times \\ \times \cos\left(-\frac{\gamma}{\pi}\sigma - \sum_{k=0}^N a_k \sin(2k\sigma(I))\right). \\ \frac{\partial y}{\partial \sigma}(\sigma(I)) = \frac{2C}{\pi \sin \sigma(I)} \exp\left(-\sum_{k=0}^N a_k \cos(2k\sigma(I))\right) \times \\ \times \sin\left(-\frac{\gamma}{\pi}\sigma - \sum_{k=0}^N a_k \sin(2k\sigma(I))\right). \end{array} \right. \quad \text{on } A'B'$$

And like

- (1) $y(\sigma(N+1)) = 1$ at the point A and $y(\sigma(1)) = -x(\sigma(1)) \tan\left(\frac{\gamma}{2}\right) = \frac{1}{C}$ at the point D for free surface AB .
- (2) $y(\sigma(N+1)) = -1$ at the point A' and $y(\sigma(1)) = x(\sigma(1)) \tan\left(\frac{\gamma}{2}\right) = -\frac{1}{C}$ at the point D' for the free surface $A'B'$, and $h = \frac{\pi}{2(N+1)}$.

We can find the contraction coefficient on the free surfaces AB and $A'B'$ by the following formula

$$\frac{1}{C} = \left\{ \begin{array}{l} 1 - h \sum_{I=1}^N \frac{2}{\pi \sin \sigma(I)} \\ \times \exp\left(-\sum_{k=0}^N a_k \cos(2k\sigma)\right) \sin\left(-\left(\frac{\pi-\gamma}{\pi}\right)\sigma - \sum_{k=0}^N a_k \sin(2k\sigma)\right). \\ 1 - h \sum_{I=1}^N \frac{2}{\pi \sin \sigma(I)} \\ \times \exp\left(-\sum_{k=0}^N a_k \cos(2k\sigma)\right) \sin\left(-\frac{\gamma}{\pi}\sigma - \sum_{k=0}^N a_k \sin(2k\sigma)\right). \end{array} \right.$$

The shape of the free surfaces is obtained by integrating the relations (3.14) and (3.15) numerically.

4. DISCUSSION OF RESULTS

We used the numerical scheme described in section 3 to compute solutions of different values of the Weber number α for several values of the angle γ . The most of the results presented here are obtained with $N = 70$.

4.1. Flow without surface tension. When the surface stress is neglected, Weber's number α tends towards the infinite and the equation of Bernoulli becomes

$$(4.1) \quad \exp(2\tau) = u^2 + v^2 = 1, \quad \text{on the free surfaces}$$

Exact analytical solutions can be computed via free streamline theory. We computed the solutions numerically using the procedure described above and our results agree with the theoretical and experimental results are given; (see Figure 4).

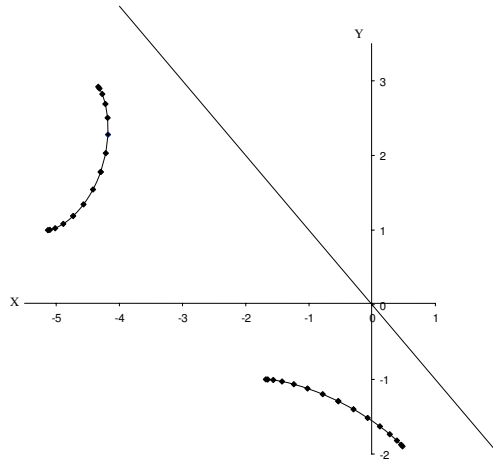
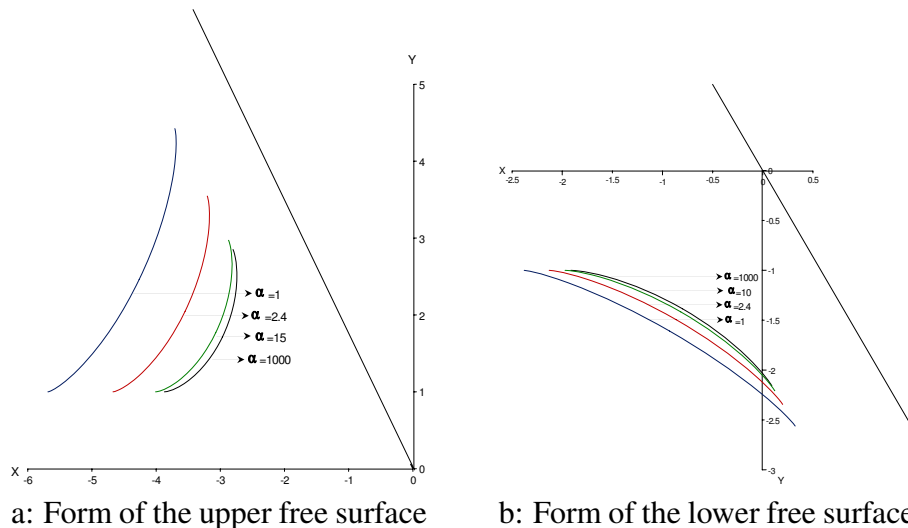


Figure 4: Numerical comparison of the free surface shape for $\gamma = \frac{\pi}{4}$

4.2. Flow with surface tension effect. When the effect of surface tension is included in the free surface condition, there is an inexact solution known. We use the numerical procedure described in section 3 to compute solutions of the problem for various values of the Weber number α , and for various values of the angle γ .

In Figure 5 and Figure 6; when $\gamma = \frac{\pi}{3}$ and $\gamma = \frac{\pi}{4}$, we showed different free surface profiles for different values of the Weber number.

when the Weber number is very large, The free surface's shape flattens and tends towards a straight line (see Figure 5 and Figure 6). For even small α , the free surface's shape was smooth without capillary waves.



a: Form of the upper free surface

b: Form of the lower free surface

Figure 5: Free surface's shape for various values of Weber number α for the angle $\gamma = \frac{\pi}{3}$

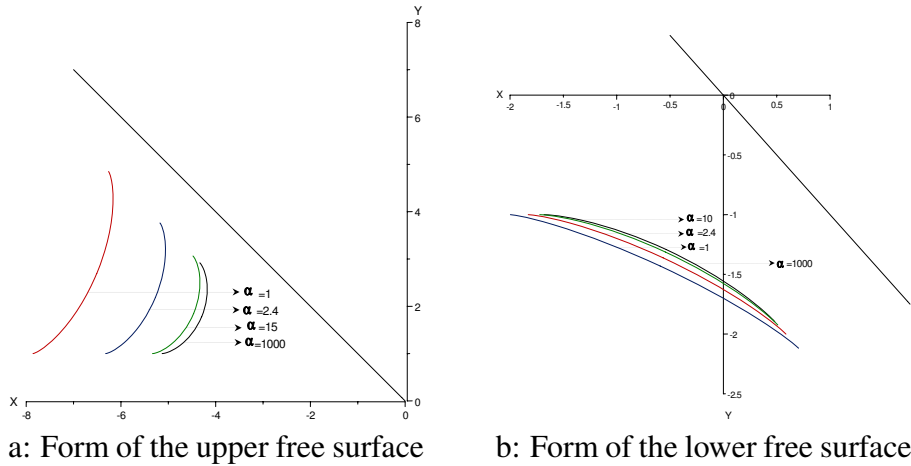


Figure 6: Free surface's shape for various values of Weber number α for the angle $\gamma = \frac{\pi}{4}$

Table 4.1: Values of the minimal Weber α_0 for some values of the angle γ and values of the Weber number α^* when the numerical scheme ceases to spare at original curve.

γ	$\frac{\pi}{2}$	$\frac{\pi}{3}$	$\frac{\pi}{4}$
α_0	0.05	0.1	0.25
α^*	25	50	100

We could compute solutions for the Weber number very small, when $\alpha \leq \alpha_0$, the algorithm converges rapidly. As an example for $\gamma = \pi/3$, we could compute the solution for all $\alpha \geq 0.1$. For each value of γ there exists a critical value α^* (see Table 4.1). For $\alpha \geq \alpha^*$ all free surface profiles for different values of $\alpha \geq \alpha^*$ and for each fixed γ are the same graphs.

The Figure 7 shows the variation of the coefficient of contraction as a function of the Weber number α .

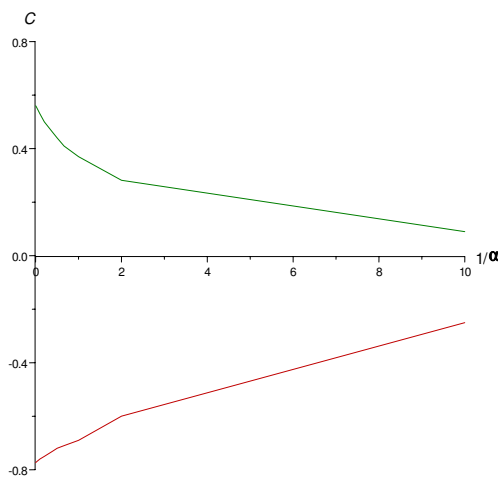


Figure 7: Variation of the contraction coefficient C according to the Weber number α for the angle $\gamma = \frac{\pi}{4}$

Table 4.2: The coefficients a_k for various values of the Weber number α and various values of the angle γ .

γ	α	a_1	a_{25}	a_{48}	a_{70}
$\frac{\pi}{4}$	10^8	-7.5×10^{-9}	6.16×10^{-12}	1.23×10^{-12}	4.25×10^{-14}
	500	-1.49×10^{-3}	1.24×10^{-6}	2.47×10^{-7}	8.46×10^{-9}
	10	-7.15×10^{-2}	7.82×10^{-5}	1.55×10^{-5}	4.7×10^{-7}
	0.01	-4.44	3.54×10^{-3}	7.57×10^{-4}	2.15×10^{-5}
$\frac{\pi}{3}$	10^7	-6.66×10^{-8}	5.47×10^{-11}	1.09×10^{-11}	3.77×10^{-13}
	100	-6.63×10^{-3}	5.63×10^{-6}	1.12×10^{-6}	3.73×10^{-8}
	50	-1.32×10^{-2}	1.15×10^{-5}	2.31×10^{-6}	7.49×10^{-8}
	0.1	-2.039	3.17×10^{-3}	6.76×10^{-4}	1.92×10^{-5}
$\frac{\pi}{2}$	10^7	-5×10^{-8}	4.1×10^{-11}	8.21×10^{-12}	2.83×10^{-13}
	250	-1.99×10^{-3}	1.66×10^{-6}	3.32×10^{-7}	1.12×10^{-8}
	5	-9.16×10^{-2}	1.22×10^{-4}	2.44×10^{-5}	7.19×10^{-7}
	0.05	-2.369	2.7×10^{-3}	5.78×10^{-4}	1.64×10^{-5}
$\frac{3\pi}{4}$	10^7	-2.49×10^{-8}	2.05×10^{-11}	4.10×10^{-12}	1.41×10^{-13}
	150	-1.66×10^{-3}	1.39×10^{-6}	2.78×10^{-7}	9.35×10^{-9}
	0.2	-6.34×10^{-1}	1.25×10^{-3}	2.66×10^{-4}	7.57×10^{-6}
$\frac{2\pi}{3}$	10^7	-3.33×10^{-8}	2.74×10^{-11}	5.47×10^{-12}	1.88×10^{-13}
	100	-3.31×10^{-3}	2.81×10^{-6}	5.62×10^{-7}	1.86×10^{-8}
	0.5	-4.22×10^{-1}	1.01×10^{-3}	2.13×10^{-4}	6.07×10^{-6}

The Table 4.2 present some values of the coefficients a_k for different values of the Weber number α and for different values of the angle γ . One finds for each value of α and for each value of γ , the coefficients a_k of the series (3.6). For fixed values of α , the coefficients a_k were found to decrease very rapidly as k increases (see Table 4.2).

5. CONCLUSION

From the above numerical results, we conclude that for all $\alpha \geq \alpha_0$ and for a fixed value of γ , there is one and only one solution. In this case the series formulation provides a good approximation. We can say that the method we adopted for the solution in this work has the advantage of converting from a two-dimensional problem to a one-dimensional problem using the conform transformations as a first stage. Then, in the second stage, we solve the problem numerically using truncation of the series technique, that enables us to obtain the results presented above. The effectiveness of the method appears in the speed of data acquisition and accuracy, due to the good convergence of the series. These results are very important, especially when they are used to complete the solution of some mathematical problems in fluid mechanics in future research, or to compare them with other problems solved in other ways.

REFERENCES

[1] A. GASMI, Numerical study of two-dimensional jet flow issuing from a funnel, *Adv. Appl. Math.*, **87**, (2014), pp. 161–169

[2] F. DIAS and J.M. VANDEN-BROECK, Potential-flow studies of steady two-dimensional jets, waterfalls, weirs and sprays, *J. Eng. Math.*, **70**, (2011), pp. 165–174

- [3] F.Z. CHEDALA, A. AMARA and M. MEFTAH, Numerical and analytical calculations of the free surface flow between two semi-infinite straights, *J. Appl. Math. Comput. Mech.*, **19**, (2020), pp. 21–32
- [4] G. BIRKHOFF and E.H. ZARANTONELLO, *Jets, wakes and cavities*, **4328**, New York Academic, (1957)
- [5] G.C. HOKING, Steady Prandtl-Batchelor flows past a circular cylinder, *Anziam J.*, **48**, (2006), pp. 165–177
- [6] G.K. BATCHELOR, *An introduction to fluid dynamics*, Cambridge University Press, (1967)
- [7] J. EGGERS and A.F. SMITH, Free streamline flows with singularities, *J. Fluid. Mech.*, **647**, (2010), pp. 187–200
- [8] J.M. CHUANG, Numerical studies on non linear free surface flow using generalized Schwartz-Christoffel transformation, *Int. J. Numer. Methods. Fluids.*, **32**, (2000), pp. 745–772
- [9] J.M. VANDEN-BROECK and A. DOAK, Nonlinear two-dimensional free surface solutions of flow exiting a pipe and impacting a wedge, *J. Eng. Math.*, **126**, (2021), pp. 1431–1434
- [10] S.J. CHAPMAN and J.M. VANDEN-BROECK, Exponential asymptotics and capillary waves, *SIAM. J. Appl. Math.*, **62**, (2002), pp. 1872–1898
- [11] S. PANDA, A study on inviscid flow with a free surface over an undulating bottom, *J. Appl. Fluid. Mech.*, **9**, (2016), pp. 1089–1096
- [12] S. PANDA, S.C. MARTHA and A. CHAKRABATI, Three-layer fluid flow over a small obstruction on the bottom of a channel, *Aanziam J.*, **56**, (2015), pp. 248–274
- [13] W. PENG and D.F. PARKER, An ideal fluid jet impinging on an uneven wall, *J. Fluid. Mech.*, **333**, (1997), pp. 231–255